

Electronic Supplementary Information

for

A supramolecular self-assembly strategy for upconversion nanoparticle bioconjugation

Yulong Sun,^{a,b,c} Wenjing Zhang,^{a,c,d} Baoming Wang,^{a,c} Xiaoxue Xu,^{a,c} Joshua Chou,^e Olga Shimoni,^{*a,b,c} Alison T. Ung,^c and Dayong Jin^{*a,b,c}

^a Institute of Biomedical Materials & Devices (IBMD), Faculty of Science, University of Technology, Sydney, Ultimo, Sydney, NSW 2007, Australia

^b ARC Research Hub for Integrated Device for End-user Analysis at Low-levels (IDEAL), Faculty of Science University of Technology, Sydney, Ultimo, NSW, 2007, Australia

^c School of Mathematical and Physical Sciences, Faculty of Science, University of Technology, Sydney Ultimo, Sydney, NSW 2007, Australia

^d Institute of Advanced Materials for Nano-Bio Application, School of Ophthalmology and Optometry Wenzhou Medical University, Wenzhou, Zhejiang 310012, P.R. China

^e School of Life Science, Advanced Tissue Regeneration and Drug Delivery Group, University of Technology, Sydney Ultimo, Sydney, NSW 2007, Australia

Contents

1	Materials and Methods.....	4
2	Preparation and Synthesis	4
2.1	<i>Synthesis of Upconversion Nanoparticle (NaYF₄: 20% Yb, 2% Er)</i>	4
2.2	<i>One-Step Ligand Exchange Synthesis of CB-UCNPs</i>	5
2.3	<i>Preparation of Direct Carboxyl-Modified Upconversion Nanoparticle (UCNPs-COOH)</i>	5
2.4	<i>EDC amide Coupling of IgG with UCNPs-COOH</i>	6
2.5	<i>Protein Modification.....</i>	6
2.5.1	<i>Synthesis of Sodium 1-adamantanecarboxylate</i>	6
2.5.2	<i>Synthesis of N-1-adamantanecarboxyl-IgG (IgG-ADC)</i>	8
2.6	<i>Self-assembly of biomolecules on the surface of CB-UCNPs</i>	9
3	Materials Characterizations	9
3.1	<i>FT-IR Spectra</i>	9
3.2	<i>Thermomechanical Analysis</i>	10
3.3	<i>X-Ray Diffraction (XRD)</i>	11
3.4	<i>X-Ray Photoelectron Spectroscopy (XPS)</i>	13
3.5	<i>Spectroscopic Analysis</i>	15
3.6	<i>TEM image</i>	16
3.7	<i>Size distributions.....</i>	16
3.8	<i>Particle Size.....</i>	17
3.9	<i>NMR Spectra.....</i>	18
4	Binding Behaviours.....	19
4.1	<i>The crystal structure of NaYF₄ Based UCNPs.....</i>	19
4.2	<i>Binding mode of OA on the surface of UCNPs</i>	19
4.3	<i>Binding mode of CB[7] on the surface of UCNPs</i>	22
4.4	<i>Quantitative Binding Amount of OA on the surface of UCNPs</i>	23
4.5	<i>Quantitative Binding Amount of CB[7] on the surface of UCNPs.....</i>	25
4.6	<i>The Mechanism and efficiency of one-step ligand exchange modification</i>	25
4.7	<i>The Mechanism of Self-assembly</i>	27
4.8	<i>Conjugation Amount Test</i>	29
4.9	<i>Conjugation Availability.....</i>	29
4.9.1	<i>Conjugation Availability of CB-UCNPs.....</i>	29
4.9.2	<i>Conjugation Availability of UCNPs-COOH</i>	30
4.10	<i>Conjugation Rate of Self-Assembly.....</i>	30

4.11	<i>The Shelf-Life of Self-Assembly Conjugation</i>	30
5	<i>In vitro</i> Cell Study	32
5.1	<i>Cytotoxicity of CB-UCNPs</i>	32
5.2	<i>Cell imaging</i>	33
5.2.1	Cell culture and immunostaining.....	33
5.2.2	Fluorescence imaging	34
6	References.....	35

1 Materials and Methods

All the starting materials and reagents were purchased from Sigma-Aldrich & Chem Supply and used as received. Unless otherwise noted, all reactions were performed under nitrogen atmosphere and in dry solvents. Cucurbit[7]uril (CB[7]) was synthesised according to a procedure reported by Day¹ and Kim². Transmission electron microscopy (TEM) images were collected on an FEI-Tecnai T20 instrument, employing an accelerating voltage of 200 kV. Fourier transform infrared (FT-IR) spectra were recorded on a Nicolet 6700 spectrometer (Attenuated Total Reflectance Method). Thermogravimetric analysis (TGA) was carried on a Simultaneous TG-DTA instrument S600 with a heating program consisting of a heating rate of 10 K/min from 373.15K to 1273.15 K under N₂. NMR Spectra were recorded on an Agilent 500 MHz NMR spectrometer. Powder X-ray Diffraction (XRD) measurements were carried out using a Bruker D8 Discover diffractometer. The radiation source was copper ($K\alpha = 1.39225 \text{ \AA}$). Particle size (dynamic light scattering) was obtained using Zetasizer Nano. X-Ray Photoelectron Spectra (XPS) were tested by Thermo ESCALAB250Xi X-ray photoelectron spectrometer. The scan number of XPS is 20 times, and the spot size is 500 μm . The Emission Spectra were carried out by our set-up instrument. The concentration of protein was examined by BCA Protein Assay Kit.

2 Preparation and Synthesis

2.1 *Synthesis of Upconversion Nanoparticle (NaYF₄: 20% Yb, 2% Er)*

The user-friendly synthesis method of the upconversion nanoparticles (NaYF₄: 20%Yb³⁺ / 2% Er³⁺) was modified from a previous report.³ Generally, monodisperse NaYF₄:Yb, Er (78/20/2 mol%), YCl₃.6H₂O (0.78 mmol), YbCl₃.6H₂O (0.20 mmol), and ErCl₃.6H₂O (0.02 mmol) in 5 mL MeOH were added to a 50 mL flask containing 6 mL Oleic Acid (OA) and 15 mL 1-Octadecene (ODE). The mixture was slowly heated to 150 °C to remove H₂O and MeOH under an argon atmosphere and maintained at 150 °C for about 30 min until a homogeneous transparent yellow solution was obtained. The system

was then cooled down to room temperature with the flowing of argon. Then 10 mL MeOH solution of NH_4F (0.148 g, 4.0 mmol) and NaOH (0.10 g, 2.5 mmol) was added, and the solution was stirred at room temperature for 1 h. The mixture was slowly heated to 110 °C to remove MeOH under argon atmosphere after MeOH evaporated, the solution was quickly heated to 300 °C and kept for 1.5 h before it was cooled down to room temperature. After the reaction, the nanoparticles were washed with the mixture solution of EtOH / MeOH / OA / cyclohexane until the cyclohexane solution turned clear. Then the nanoparticles were dispersed and stored in cyclohexane. These nanoparticles were characterised by TEM, DLS (particle size), TGA, emission spectrum, XRD, XPS, and FT-IR.

2.2 *One-Step Ligand Exchange Synthesis of CB-UCNPs*

The CB[7] stabilised UCNPs were synthesized according to the modified method reported by Lu et.al.³ In brief, 10 μL of a UCNPs solution (10 mg/mL in cyclohexane) were added into 100 μL organic solvent (e.g., chloroform) and mixed with 300 μL of CB[7] aqueous solution with different concentrations. The mixture was shaken and incubated for 12h, and the water layer was collected and centrifuged at 13,000 rpm for 5 min. Then, the particulate was dispersed and centrifuged in water to remove extra free CB[7] molecules. The wash step was repeated at least three times. These nanoparticles are characterized by TEM, DLS (particle size), TGA, emission spectrum, XRD, XPS, FT-IR, and NMR spectrum.

2.3 *Preparation of Direct Carboxyl-Modified Upconversion Nanoparticle (UCNPs-COOH)*

The carboxyl-modified upconversion nanoparticles were synthesised according to the research article of Tan⁴. 3,4-dihydroxyhydrocinnamic acid (50 mg) was dissolved in 5 mL of tetrahydrofuran (THF) and mixed with the solution of OA-UCNPs (15 mg, in 2 mL of THF). The reaction was incubated for 5 h at

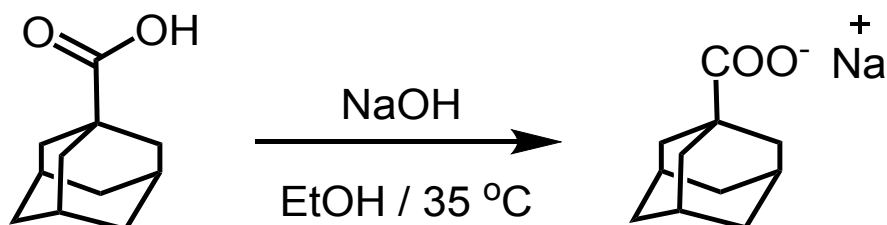
50 °C. After the reaction, 200 μ L of NaOH solution (0.5 M) was added into the mixture to obtain the precipitate, which was collected by centrifuge and redispersed in H₂O.

2.4 EDC amide Coupling of IgG with UCNPs-COOH

UCNPs-COOH, (100 μ g) was dispersed in 500 μ L of H₂O. Meanwhile, 1.0 mg IgG powder was dissolved in 500 μ L of MES buffer and mixed with UCNPs-COOH solution. Then, EDC (2.5 mg) was added to the mixture. The reaction was stirred at 4 °C overnight. The sample was collected by centrifuge (13,000 rpm, 30 min). The precipitate was washed with H₂O.

2.5 Protein Modification

2.5.1 Synthesis of Sodium 1-adamantanecarboxylate



Scheme S1. Synthesis of SA.

200 mg of 1-adamantanecarboxylic acid was dissolved in EtOH (5 mL), and 44.4 mg of NaOH was dissolved in EtOH (5 mL). Both two EtOH solutions were mixed and stirred at 35 °C overnight. The solvent was removed by vacuum to get white powder. The yield is 95.5 %. ¹H NMR (500 MHz, 25 °C, D₂O) δ 1.57 (q, 6H), 1.67 (d, 6H), 1.84 (s, 3H). ¹³C NMR (125 MHz, 25 °C, D₂O) δ 30.72, 38.86, 42.12, 44.80, 190.96. FT-IR (ATR): 2901, 2847, 1540, 1450, 1400, 760, 677 cm⁻¹. These spectra are shown in Figure S1-S3.

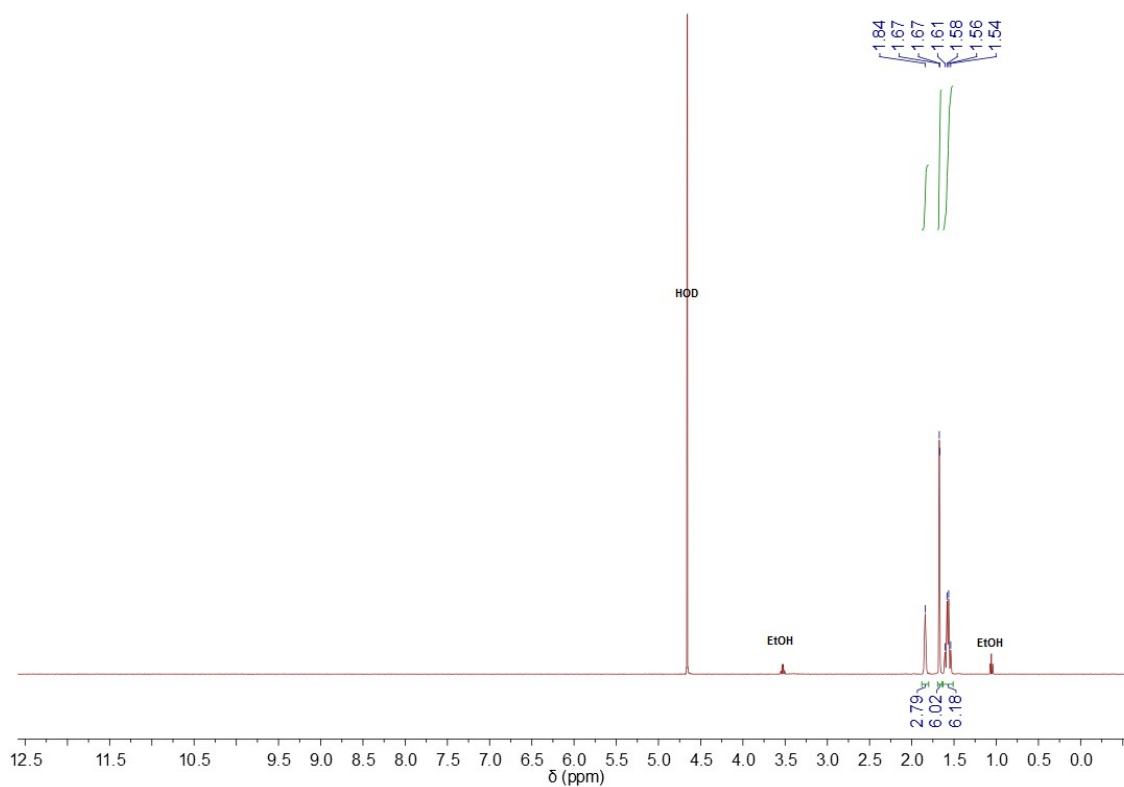


Figure S1. ^1H NMR spectrum of SA in D_2O at 25°C .

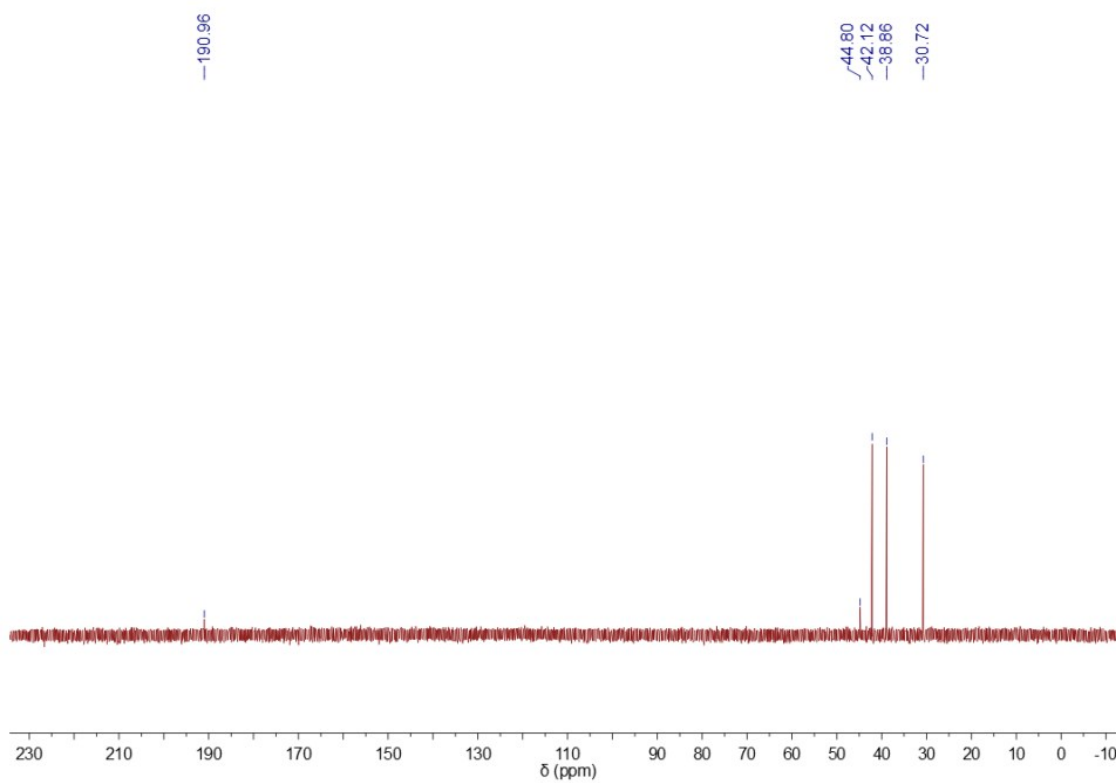


Figure S2. ^{13}C NMR spectrum of SA in D_2O at 25°C .

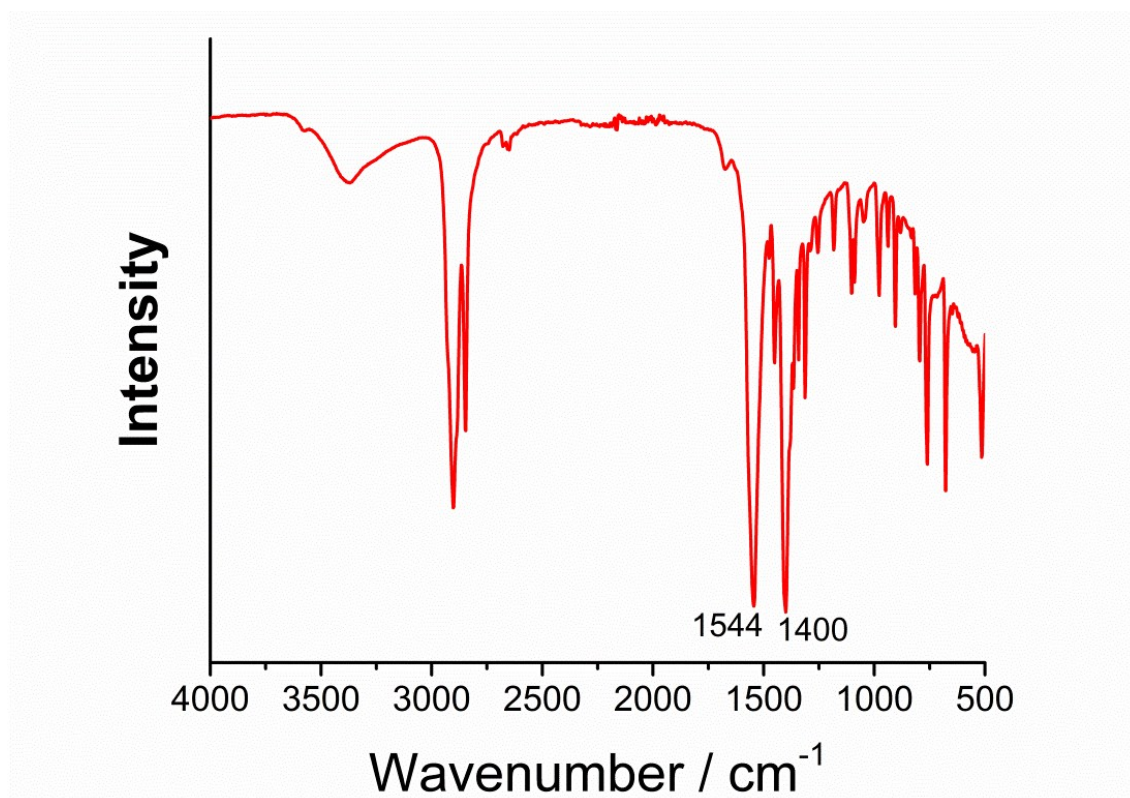
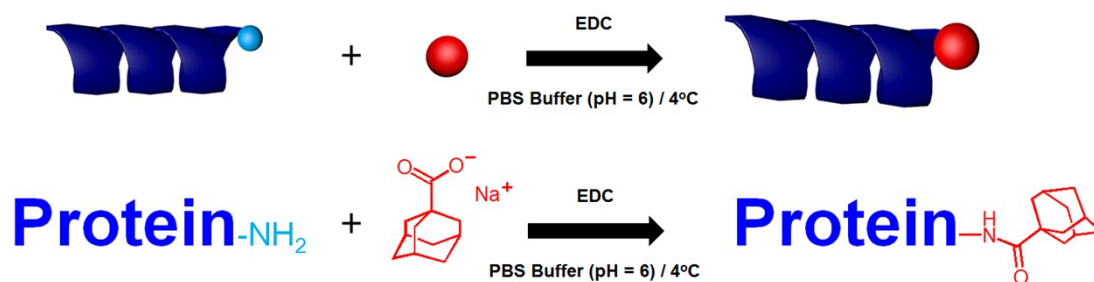


Figure S3. FT-IT spectrum of SA.

2.5.2 Synthesis of *N*-1-adamantanecarboxyl-IgG (IgG-ADC)

The procedure for the synthesis of SA-modified IgG is according to the modified process of Fragoso's report (**Scheme S2**).⁵ The mixture including 1 mg IgG powder (Mw = 150,000), 5 mg of SA and 2.5 mg of 1-ethyl-3-(3-dimethylaminopropyl)carbodiimide (EDC) was dissolved in 5 mL of 50 mM potassium phosphate buffer (pH 6). The reaction was stirred overnight at 4-5 °C. The solution was concentrated and separated by a centrifugal filter. Due to the high concentration of SA and EDC, few positions, like lysine residues, may also be modified with ADC.



Scheme S2. Synthesis of 1-adamantanecarboxylate-modified IgG from rabbit.

2.6 Self-assembly of biomolecules on the surface of CB-UCNPs

The mixture of CB-UCNPs (0.1 mg) and biomolecules (1 mg) was incubated in a suitable buffer and stirred at 4 °C for 24h. The mixture was centrifuged at 14,000 rpm for 5 mins at 4°C. The participants were washed with the same buffer and centrifuged again. The sample was dispersed in a buffer for further test.

3 Materials Characterizations

3.1 FT-IR Spectra

FT-IR spectra of free OA (red) and OA-UCNPs (blue) were shown in **Figure S4**. In the frequency of free OA, the ν_{st} (O-H) stretching from the carboxylic acid group was shown as a broad range from 3300 cm^{-1} to 2500 cm^{-1} because of the hydrogen bond. The range of C=O from COOH is from 1800 cm^{-1} to 1650 cm^{-1} . Specifically, when the COOH is connected with an aliphatic group, the typical range is from 1725 cm^{-1} to 1700 cm^{-1} . In **Figure S4**, the sharp peak of ν_{st} (C=O) stretching of OA was displayed at 1708 cm^{-1} , it also indicated that COOH group was involved in the structure. In the spectrum of OA-UCNPs, the H-bonded broad peak (3300 cm^{-1} ~ 2500 cm^{-1}) was disappeared, compared with the free OA spectrum. The ν_{st} (C=O) stretching was splitted into two peaks, and they shifted to

1547 cm^{-1} (asymmetric) to 1461 cm^{-1} (symmetric), respectively. It means the carboxylic acid groups in the OA had already changed to carboxylate ($-\text{COO}^-$) after modified on the surface of upconversion nanoparticles rather than carboxylic acid ($-\text{COOH}$).

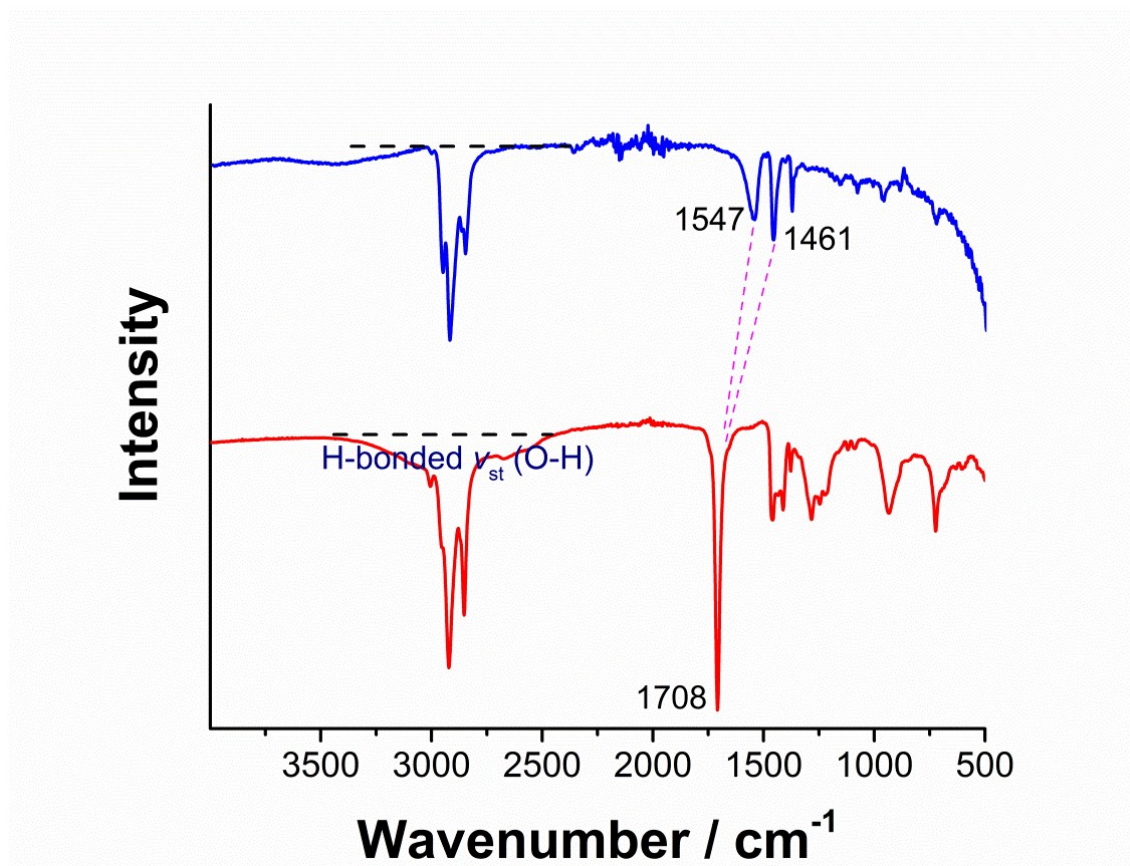


Figure S4. FT-IR spectra of OA (red) and OA-UCNPs (blue).

3.2 Thermomechanical Analysis

Before exchanging the ligand on the surface of UCNPs, OA covered on the surface to stabilise and protect the nanoparticles³. The TGA and DTGA curves (**Figure S5**) of free OA showed all the free OA could be removed before 300 °C and the weight loss temperature is 280 °C. After OA modified on the surface of bare UCNPs (**Figure S6**), the temperature of removal is higher than free OA. It means that OA is binding on the surface of UCNPs.

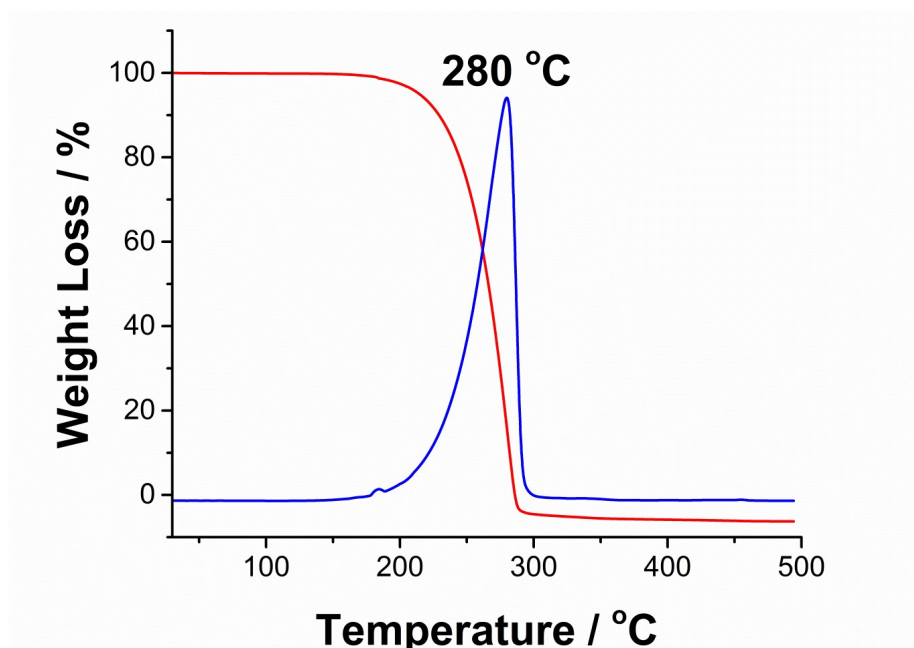


Figure S5. The TGA (red) and DTGA (blue) curves of OA.

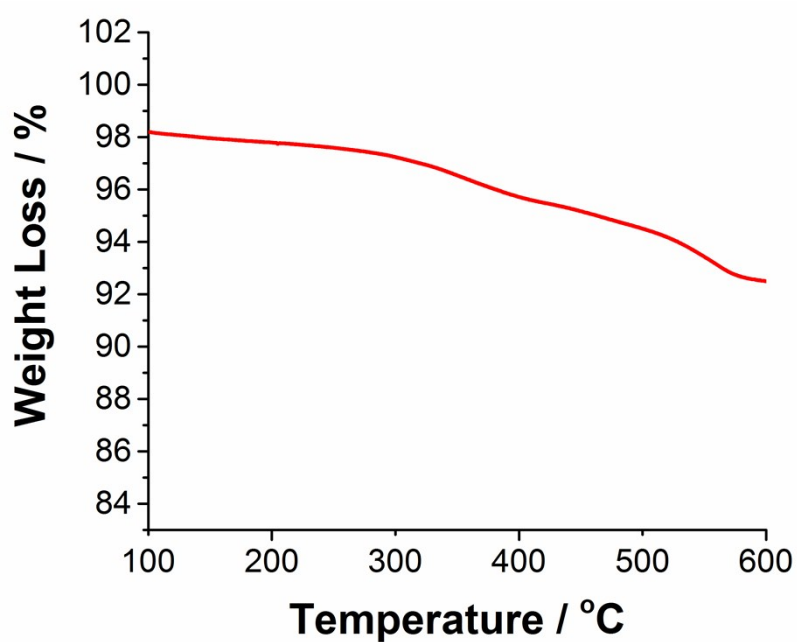


Figure S6. The TGA curve of OA-UCNPs.

3.3 X-Ray Diffraction (XRD)

Figure S7 showed the XRD patterns of β -NaYF₄ nanocrystals co-doped with 2% Er³⁺ and 20 % Yb³⁺ (OA-UCNPs), with the standard XRD patterns of hexagonal phase NaYF₄ (JCPDS: 00-016-0334) and

NaYbF₄ (JCPDS: 00-027-1427). After ligand exchange, the XRD Patterns of CB-UCNPs still kept the hexagonal phase.

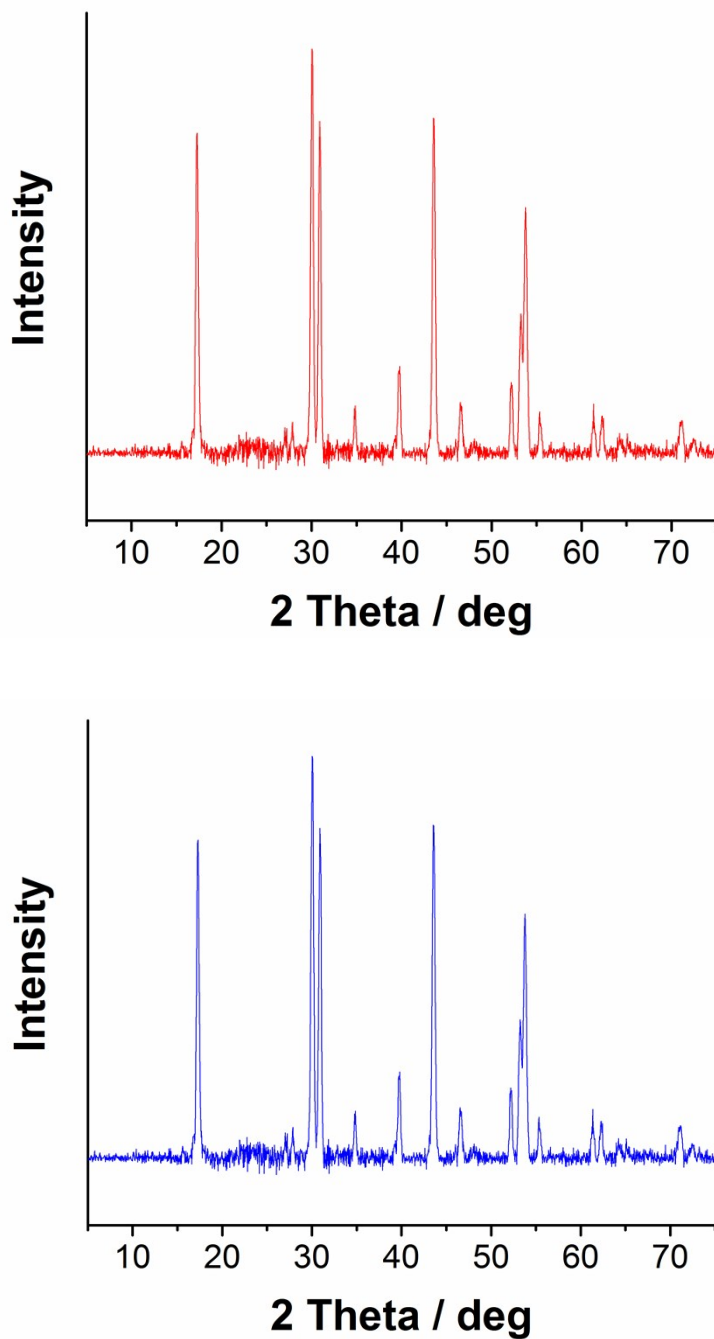


Figure S7. The XRD patterns of OA-UCNPs (β -NaYF₄: 2%Er³⁺/20%Yb³⁺@OA) (red) and CB-UCNPs(β -NaYF₄: 2%Er³⁺/20%Yb³⁺@CB[7]) (blue).

3.4 X-Ray Photoelectron Spectroscopy (XPS)

In the O1s region, only one O1s peak was shown in **Figure S8**. It proves only one type of oxygen in the system. Further evidence illustrated both two carbon-oxygen bonds in the carboxylic group of OA were equalised after modified on the surface of β -NaYF₄ crystal because of resonance. **Figure S9** showed that there are two kinds of oxygens on the surface. However, CB[7] molecule is symmetry, all of the oxygens should be the same. So it further proves that the CB[7] modified on the surface of UCNPs, because parts of molecules moved to another position.

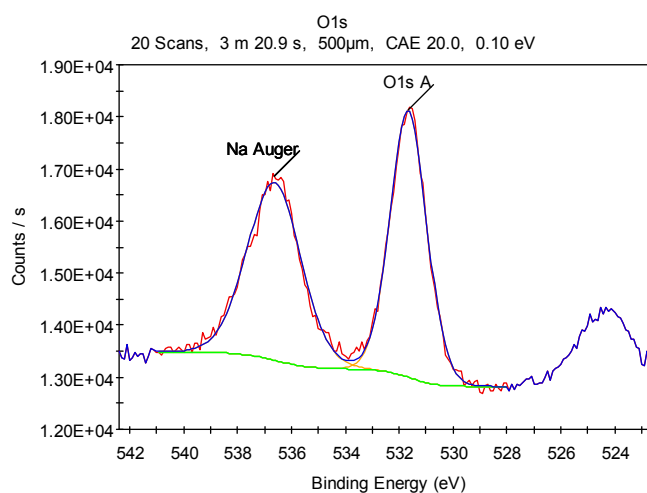


Figure S8. XPS Spectrum (O1s) of OA-UCNP.

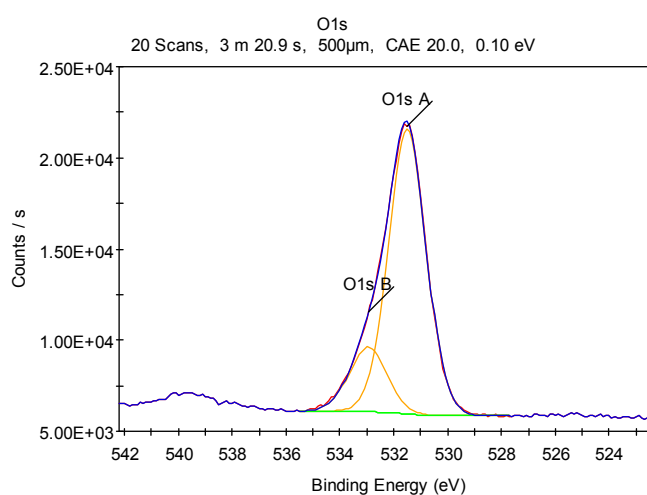


Figure S9. XPS Spectrum (O1s) of CB-UCNP.

In **Figure S10**, the peak B also proves two carbon-oxygen bonds are the same because of resonance. There are three kinds of carbon in free CB[7] after modified on the surface of the nanoparticle (**Figure S11**), these peaks were split, because of the effect from the surface of UCNPs.

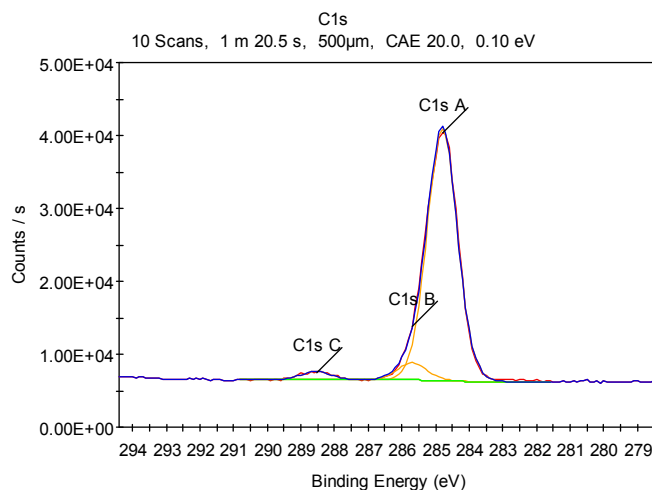


Figure S10. XPS Spectrum (C1s) of OA-UCNP.

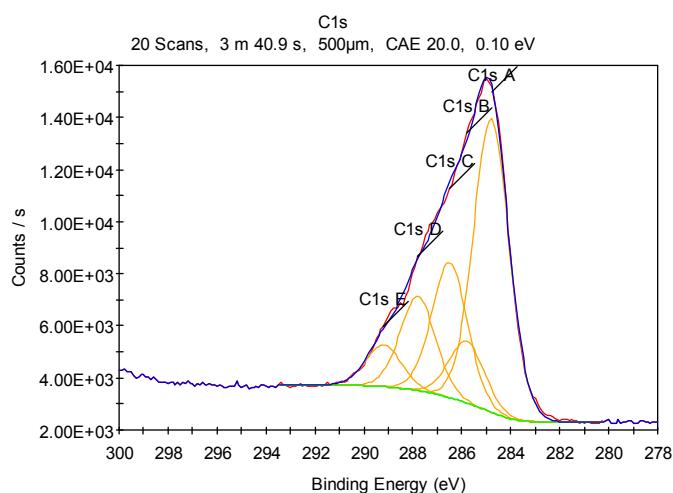


Figure S11. XPS Spectrum (C1s) of CB-UCNP.

After exchanged with CB[7], nitrogen was found as a new element from CB[7] on the surface. In addition, the only one peak from free CB[7] was also split because of the surface of UCNPs. (**Figure S12**)

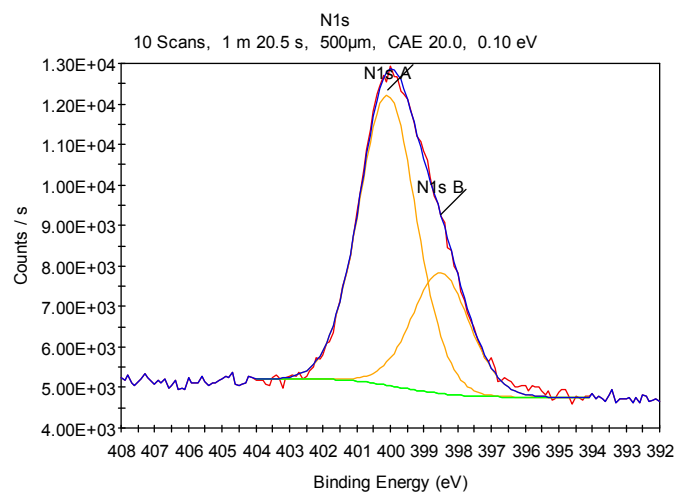


Figure S12. XPS Spectrum (N1s) of CB-UCNP.

3.5 Spectroscopic Analysis

The emission of CB[7] modified NaYF₄ nanocrystal co-doped with 20% Yb and 2% Er was shown in **Figure S13**.

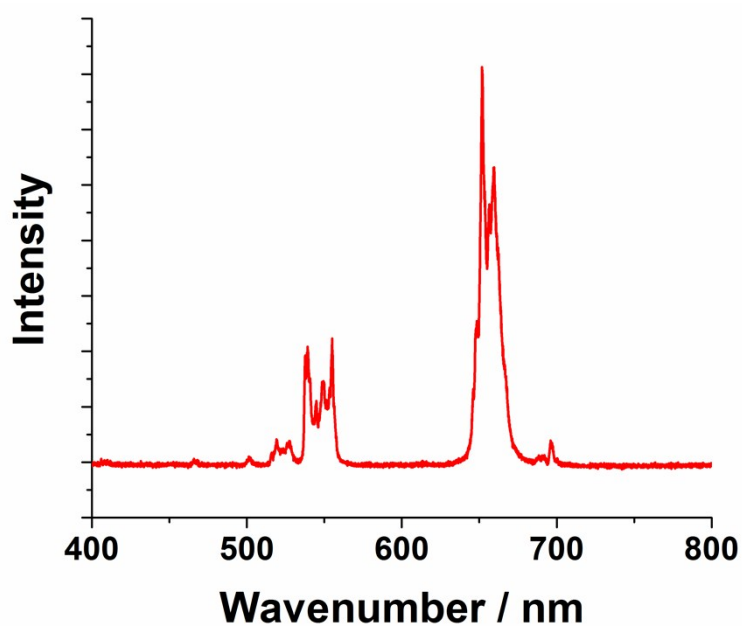


Figure S13. The emission spectrum of CB[7]-functional NaYF₄ nanocrystal co-doped with 20% Yb and 2% Er.

3.6 TEM image

The TEM image of OA-UCNPs was shown in **Figure S14**. The size of the particle is around 37 nm.

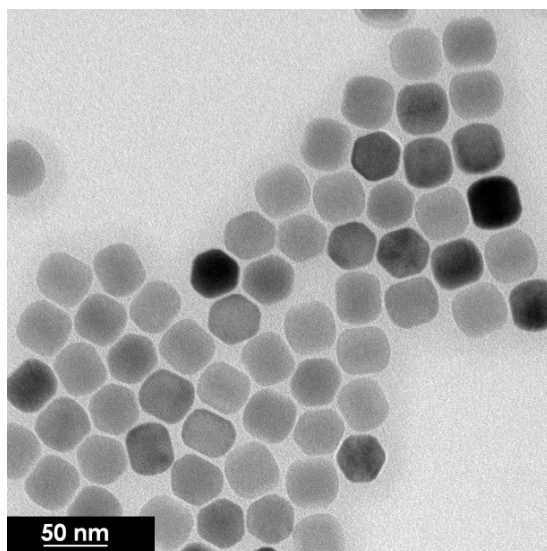


Figure S14. The TEM image of OA-UCNPs.

3.7 Size distributions

The size distribution of OA-UCNPs and CB-UCNPs are shown in **Figure S15** and **Figure S16**.

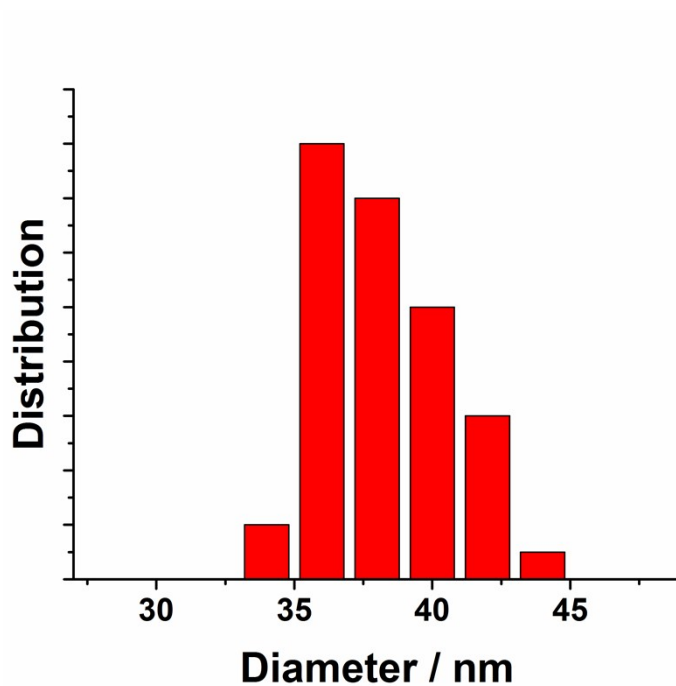


Figure S15. The size distribution of OA-UCNPs.

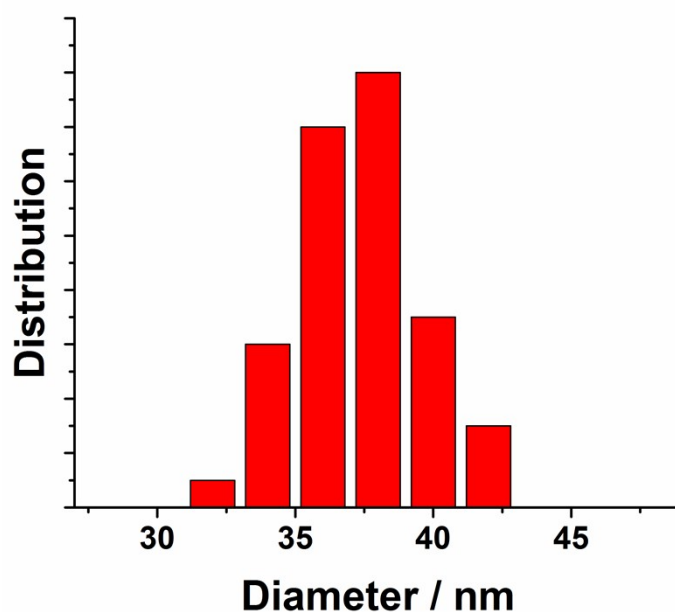


Figure S16. The size distribution of CB-UCNPs.

3.8 Particle Size

DLS was used to calculate the average size of OA-UCNPs in cyclohexane and CB-UCNPs in water. The average particle size of OA-UCNPs in cyclohexane (**Figure S17**) is ca. 37 nm. The size distribution generated by DLS is a number distribution. After exchanged with CB[7], the average particle effective size of CB-UCNPs was ca. 78 nm (**Figure S18**). It is understandable because the DLS measures the hydraulic diameter of the nanoparticles rather than the actual size. The DLS results would be different for the same batch nanoparticles when they are in a different solvent and with different surface modifications.

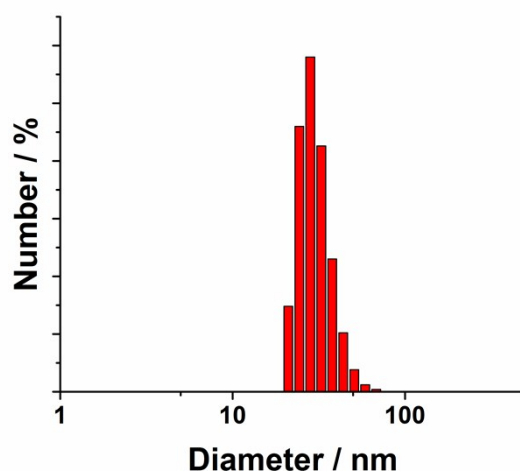


Figure S17. The size of OA-UCNPs in cyclohexane.

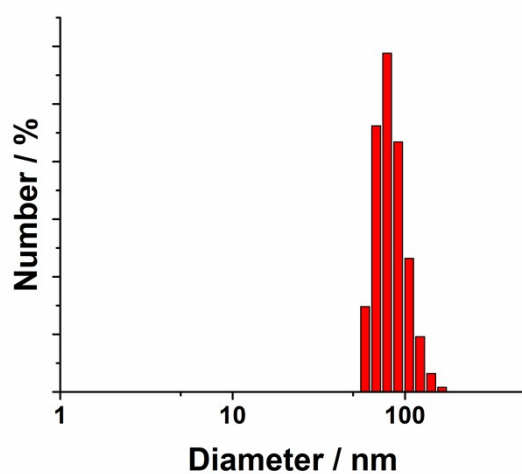


Figure S18. The size of CB-UCNPs in water.

3.9 NMR Spectra

^1H NMR of CB-UCNPs was shown in **Figure S19**. It also proves that CB[7] had already entirely replaced OA from the surface of OA-UCNPs.

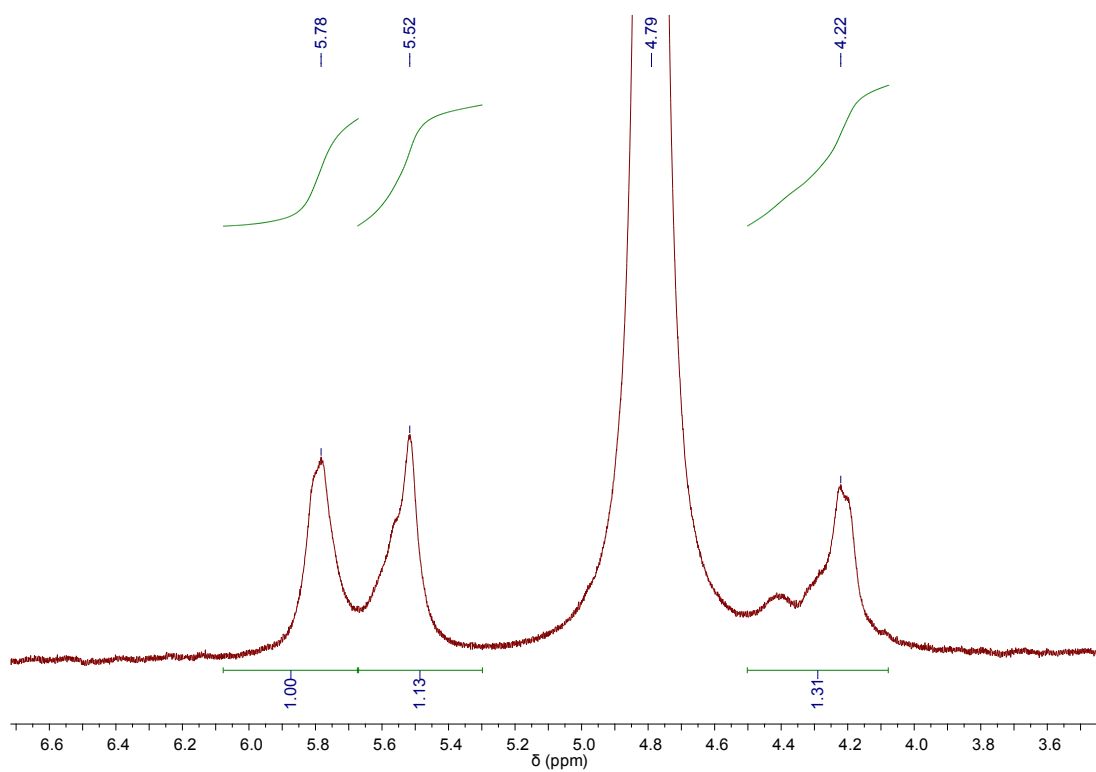


Figure S19. ^1H NMR Spectrum of CB-UCNPs in D_2O at 25 °C.

4 Binding Behaviours

4.1 The crystal structure of NaYF₄ Based UCNPs

Figure S20 shows β -NaYF₄ nanocrystal units which consist of the {001} facets at the ends and identical {100} facet around the cylinder sides. The Y³⁺ atoms form equilateral triangles with a length of 5.96 Å in the relaxed {001} surface, while rectangles are detected in the {100} surface with a shorter length of 3.53 Å.⁶

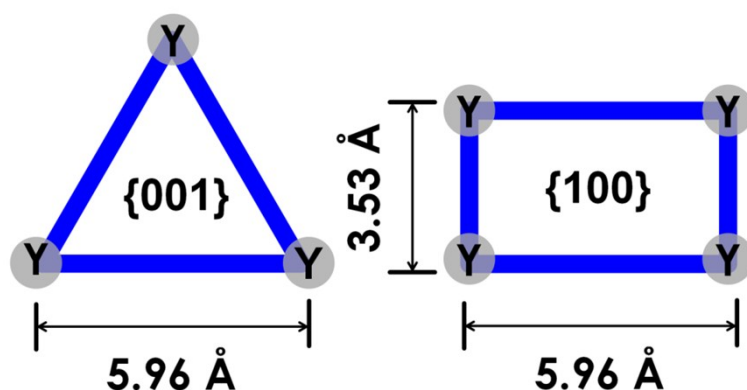


Figure S20. β -NaYF₄ nanocrystal units: the distance between two adjacent Y³⁺ atoms is 5.96 Å in {001} facet (left); the two types of distances between two adjacent Y³⁺ atoms are 5.96 Å and 3.53 Å, (right).

4.2 Binding mode of OA on the surface of UCNPs

Figure 21a shows the structure of OA. According to the characterisation of OA-UCNP's surface, the form of OA is OA⁻ rather than OA. Due to the resonance of OA⁻ (**Figure 21b**), both of the C-O bonds are the same, 127 pm, and shown in **Figure 21c**. We predicted all the binding potentials which were shown in **Table S1** and **Table S2**. Compared with bond energies, we considered most of OA⁻ on the surface is binding mode 1 and 5 in **Table S2**. The main text showed our predicted binding mode in **Figure 2**.

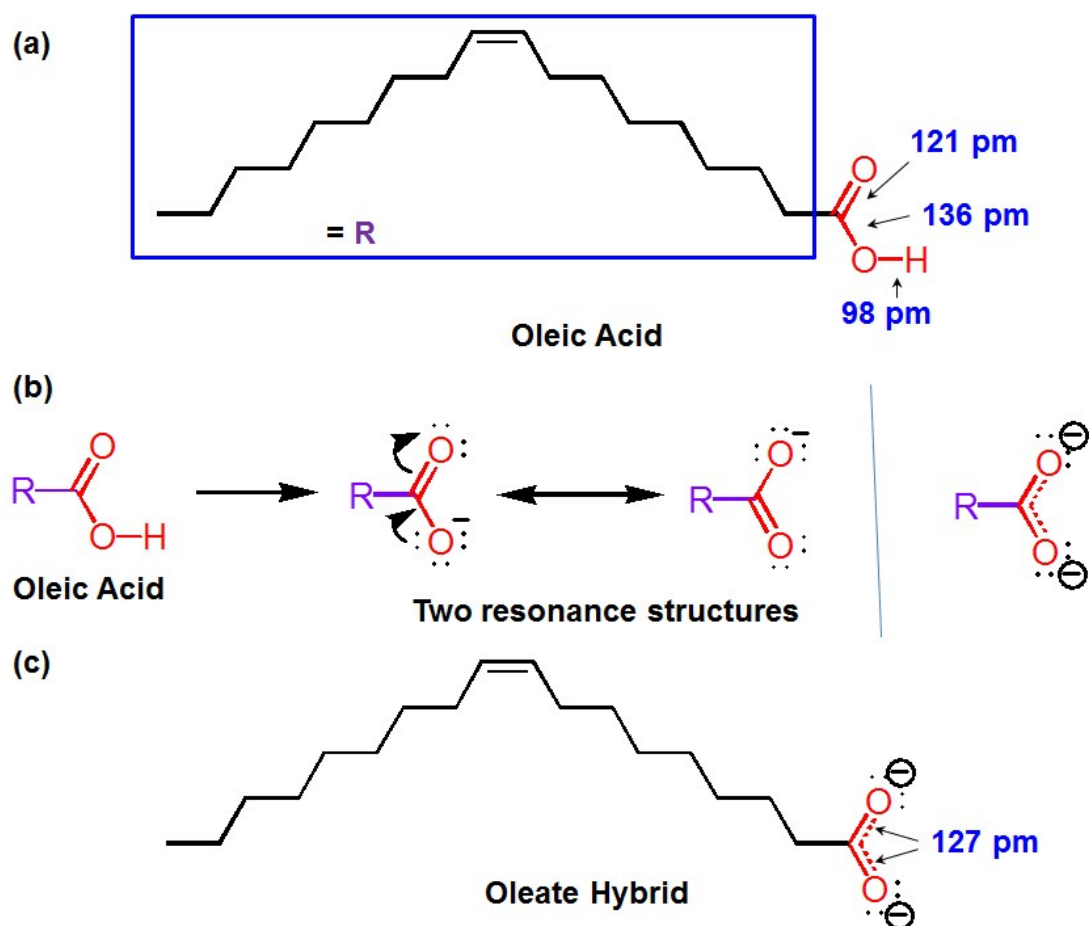


Figure S21. The structure of OA.

Table S1. Summary of Binding Mode of OA on the surface of the β -NaYF₄ crystal.

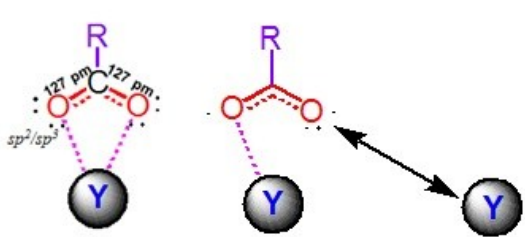
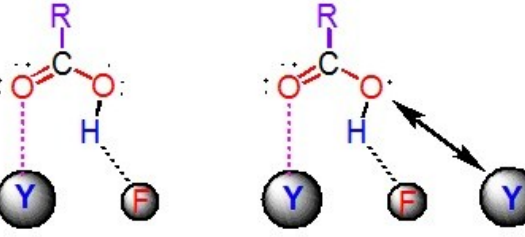
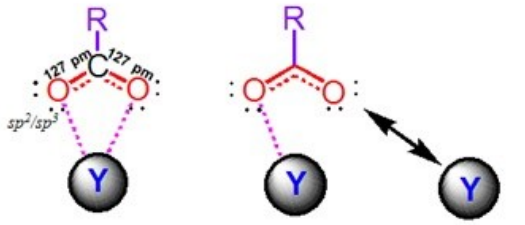
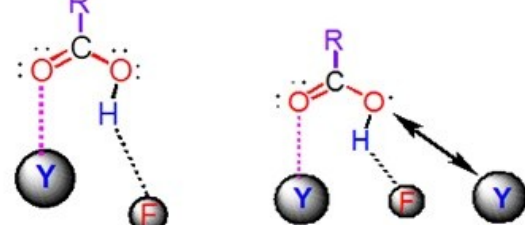
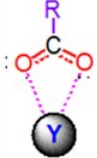
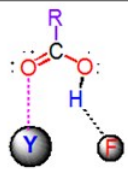
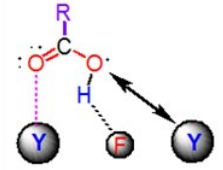
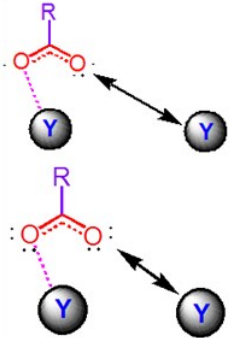
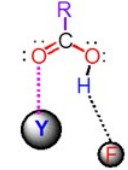
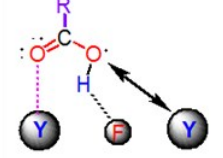
{001}		
{100}		

Table S2. Binding Mode of OA on the surface of NaYF₄.

Number	Crystal Surface Plant	Molecular Structure	Binding Mode	Model
1	001	Oleate Hybrid	One Y atom	
2	001	Oleate Hybrid	Two Y atom	
3	001	Oleic Acid	One Y atom	
4	001	Oleic Acid	Two Y atom	
5	100	Oleate Hybrid	One Y atom	
6	100	Oleate Hybrid	Two Y atom	
7	100	Oleic Acid	One Y atom	
8	100	Oleic Acid	Two Y atom	

4.3 Binding mode of CB[7] on the surface of UCNPs

The structure of CB[7] was shown in **Figure S22**. Both sides of CB[7] have seven ketones, which form a substantial π electronic cloud. So CB[7] processes very high binding with NaYF₄ crystal surface because of charge transfer interactions. The binding mode of CB[7] on the surface of the NaYF₄ crystal is shown in **Figure S23**.

According to the previous reference⁷, the binding constant (log K) of carboxylic acid with Y atom is from 1.97 to 1.42. About CB-UCNPs, seven ketones from CB[7] bind with three Y atoms. It means more than two ketones share one Y atom. In this situation, the binding constant (logK) of two ketones with one Y atom is 7.19. In addition, the multiple binding sites of CB[7] with Y atoms can increase the binding constant. So the binding constant of CB[7] with Y atom is much higher than OA.

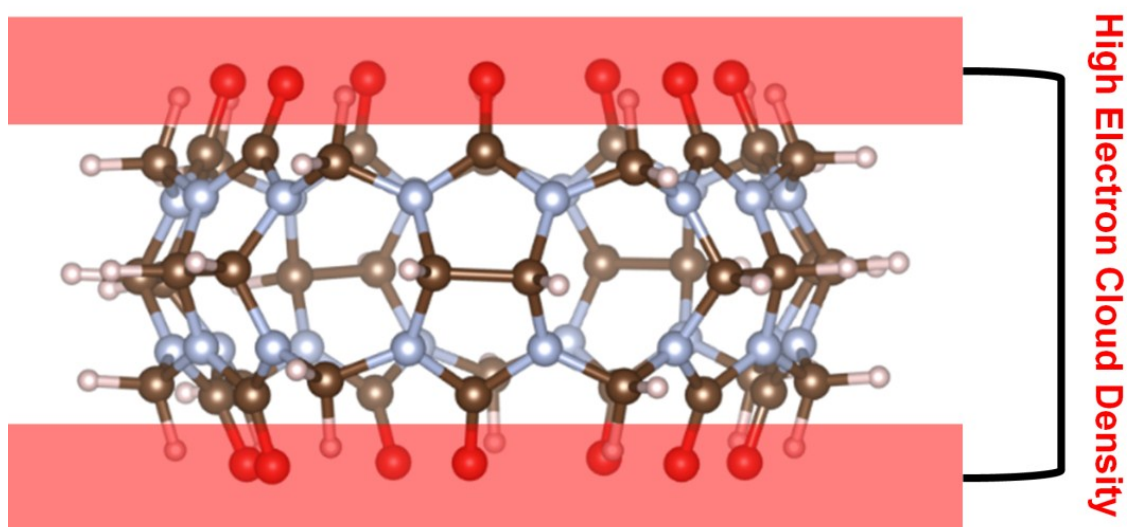


Figure S22. The structure of CB[7].

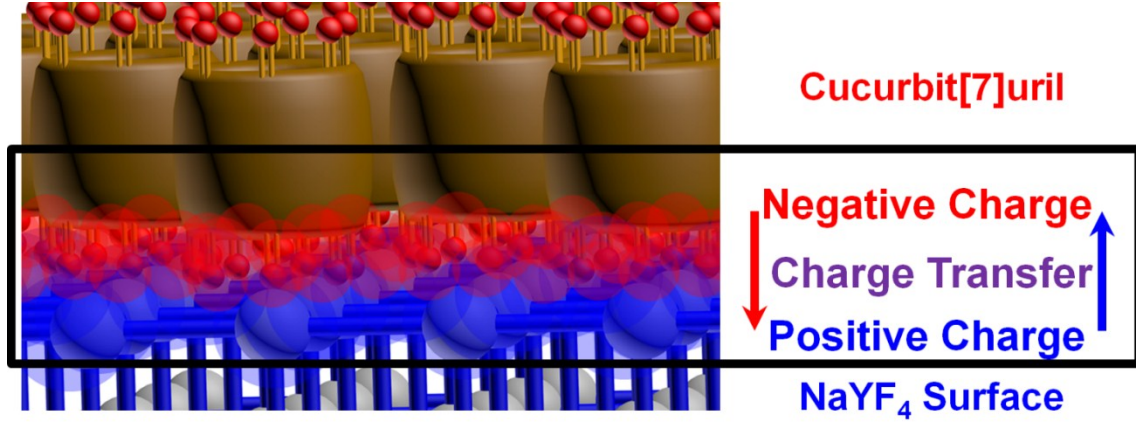


Figure S23. The binding mechanism of CB[7] on the surface of NaYF₄.

4.4 Quantitative Binding Amount of OA on the surface of UCNPs

According to the binding mode above, the OA molecules form 1:1 binding with Yttrium atoms on the surface of UCNPs.

So, the coverage of OA on the surface of UCNP is

$$\text{Coverage rate} = \frac{\text{the amount of OA molecules}}{\text{the amount of Yttrium atoms on the surface of UCNPs}} \% \quad (1)$$

The weight loss of OA-UCNPs shows the percentage of OA molecules. Besides, the number of Yttrium atoms is based on the size of UCNPs, which is measured from TEM image. The process of calculation is displayed below.

The **total volume** of UCNP (V_u) is

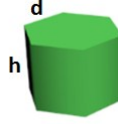
$$V_u = \frac{m_u}{\rho_u} \quad (2)$$

where the density of upconversion nanoparticle (ρ_u) is 4.2 g/cm³, m_u is the mass of UCNP.

The volume of single particle (V_s) is

$$V_s = \frac{3\sqrt{3}}{2} d^2 h \quad (3)$$

where d is the length of a nanoparticle size on {001}, h is the height of a {100} crystal face of a nanoparticle.



The numbers of nanoparticle (N) is

$$N = \frac{V_u}{V_s} = \frac{m_u / \rho_u}{\frac{3\sqrt{3}}{2}d^2h} = \frac{2m_u}{3\sqrt{3}d^2h\rho_u} \quad (4)$$

The numbers of Yttrium atom on the surface of nanoparticles

The surface area of single nanoparticle (S_s) is

$$S_s = 3\sqrt{3}d^2 + 6hd \quad (5)$$

where d is the length of a nanoparticle size on {001}, h is the height of a {100} crystal face of a nanoparticle.

The occupied area of a Y atom on {001} (Eq. S6) or {100} (Eq. S7) crystal plate is

$$S_{\{001\}} = \frac{\sqrt{3}}{2}a^2 \quad (6)$$

$$S_{\{100\}} = ab \quad (7)$$

where a and b are the distance between two atoms in different crystal plates, which is shown in **Figure S20**.

The surface numbers of Y atoms (N_s) on a nanoparticle is

$$N_s = \frac{6d^2}{a^2} + \frac{6hd}{ab} = \frac{6d^2b + 6ahd}{a^2b} \quad (8)$$

The amount of Y atoms (N_Y) is

$$N_Y = N_s \times N = \frac{2m_u}{3\sqrt{3}d^2h\rho_u} \times \frac{6d^2b + 6ahd}{a^2b} = \frac{4dm_u(db + ah)}{\sqrt{3}d^2h\rho_u a^2b} \quad (9)$$

The amount of OA molecules (N_{OA}) is

$$N_{OA} = n_{OA} \times N_A = \frac{m_{OA}}{M_{OA}} \times N_A \quad (10)$$

The coverage rate of OA on the surface of UCNP is

$$\text{Coverage rate} = \frac{N_{OA}}{N_Y} = \frac{\sqrt{3}d^2 h \rho_u a^2 b m_{OA} N_A}{4 d m_u (db + ah) M_{OA}} \quad (11)$$

So, the coverage of OA-UCNPs is 54.6%.

4.5 Quantitative Binding Amount of CB[7] on the surface of UCNPs

According to the binding mode of CB[7] on the surface of UCNPs, we found each CB[7] molecule can occupy three Yttrium atoms. So the coverage of CB[7] on the surface of UCNPs is

$$\text{Coverage rate} = \frac{3 \times \text{the amount of CB molecules}}{\text{the amount of Yttrium atoms on the surface of UCNPs}} \% \quad (12)$$

The process of calculation of CB-UCNPs is similar to the OA one above.

So, the coverage of OA-UCNPs is 50.1%.

4.6 The Mechanism and efficiency of one-step ligand exchange modification

Before exchanged on the surface of OA-UCNPs, the ligands followed dynamic equilibrium according to chemical kinetics. The rate ($K_{\text{falling off}}$) of molecular falling off from the surface is almost equal to the rate (K_{binding}) of molecular binding on the surface at the same time. Both of the rates are practically equal.

$$K_{\text{falling off}} = K_{\text{binding}}$$

After at least 12h shaking, all of the nanoparticles were extracted from cyclohexane layer (**Figure S24**). These emission spectra before and after exchange are shown in **Figure S25**.

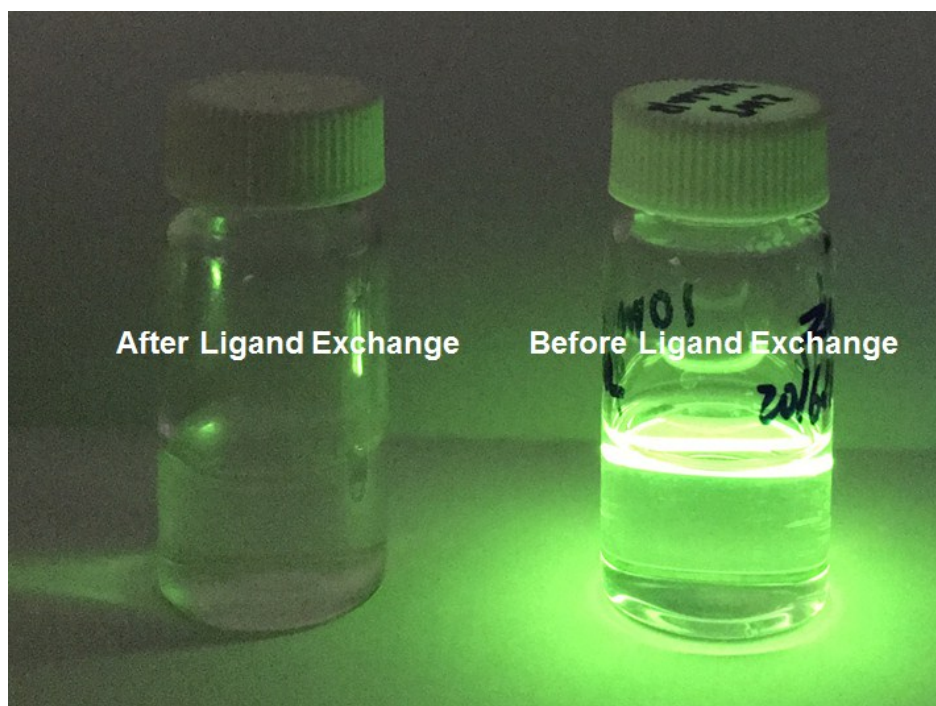


Figure S24. Comparison of visible emission between the cyclohexane layer before (a) and after (b) ligand exchange with CB[7] solution under 980 nm laser.

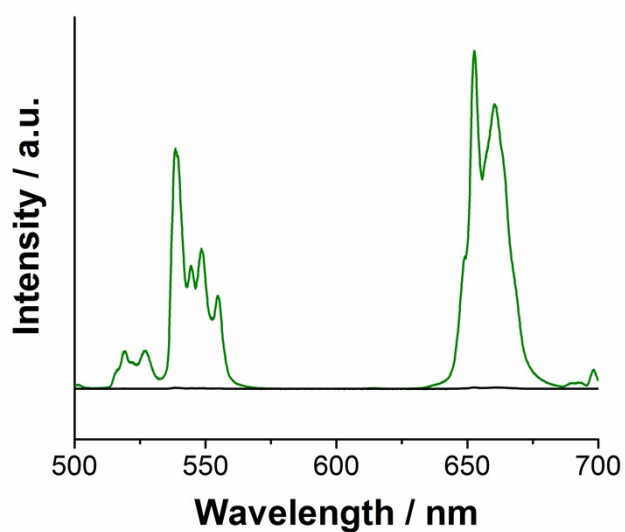


Figure S25. The emission spectra of cyclohexane layer: before exchange (green) and after exchange (black) under 980 nm laser.

4.7 The Mechanism of Self-assembly

Cucurbituril molecules have a non-polar cavity and two polar portals. The fixed negative charge is formed on both sides. Typically, the guests of cucurbiturils have one of the following properties at least: i). positive charge; ii). hydrophobic; iii). the fitting size.

The amino acids have to bind with CB[7], because of the charge transfer between the cationic amino group and negative portals. The binding constants and test conditions of amino acids were shown in **Figure S26** and **Table S3**, which values are from 10^1 M^{-1} to 10^6 M^{-1} .⁸⁻¹¹ However, the highest binding of amino acid (Phe) is still much lower than 1-adamantanecarboxylic acid ($3.23 \times 10^8 \text{ M}^{-1}$). According to selective binding theory,¹² CB[7] will choose 1-adamantanecarboxylic acid rather than amino acids in general proteins. The binding mode is shown in Figure S27.

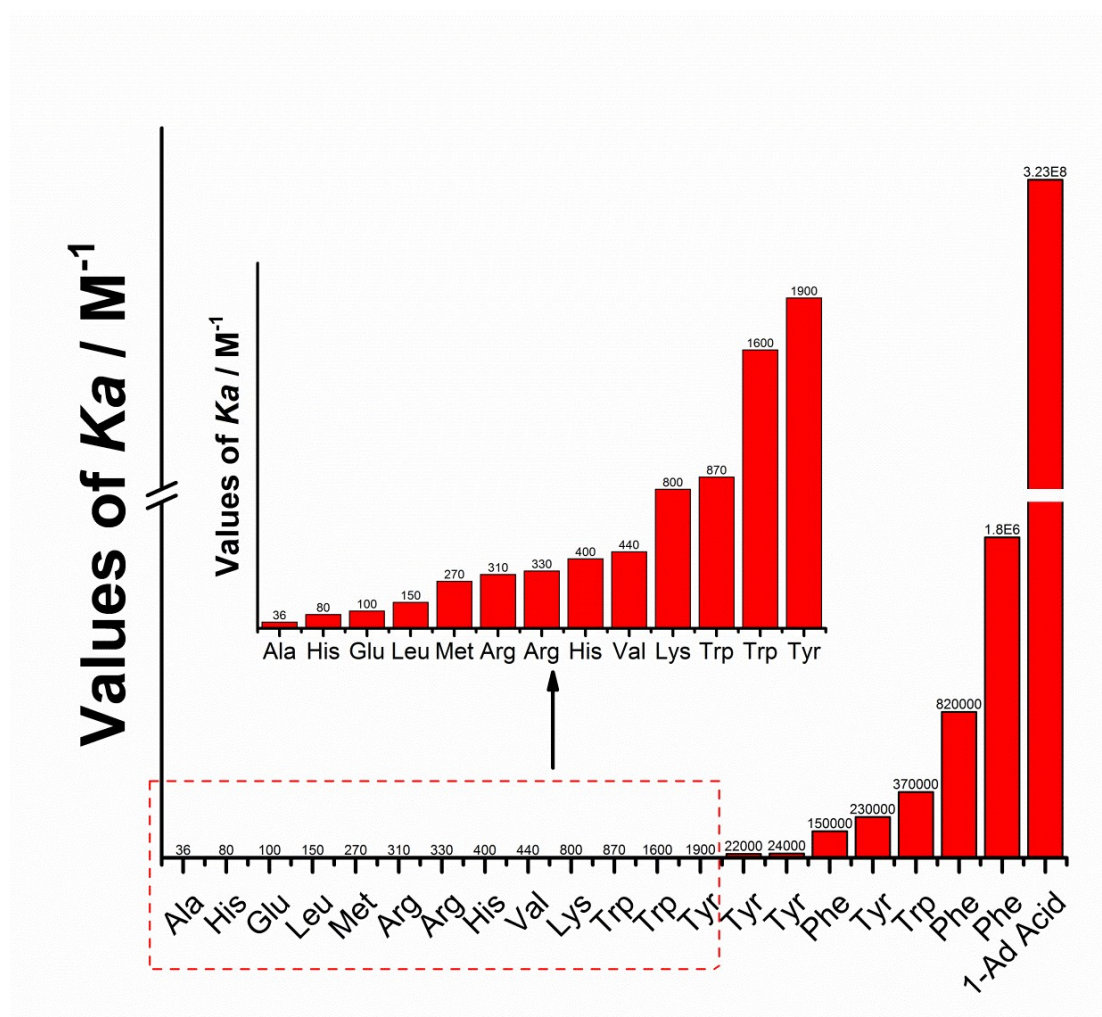


Figure S26. Binding contrasts of amino acids and 1-admantanecarboxylic acid with CB[7].

Table S3. Binding constants of amino acids and 1-adamantanecarboxylic acid with CB[7].

Guest molecule	Ka (M ⁻¹)	Method	Conditions	Ref.
Ala	3.6 × 10	UV titration		18 ⁸
His	8.0 × 10	UV titration		18 ⁸
Glu	1.0 × 10 ²	UV titration		18 ⁸
Leu	1.5 × 10 ²	UV titration		18 ⁸
Met	2.7 × 10 ²	UV titration		18 ⁸
Arg	3.1 × 10 ²	Fluorescence titration	10 mM NH ₄ OAc, pH = 6, 25°C	19 ⁹
Arg	3.3 × 10 ²	ITC	10 mM NH ₄ OAc, pH = 6, 30°C	19 ⁹
His	4.0 × 10 ²	Fluorescence titration	10 mM NH ₄ OAc, pH = 6, 25°C	19 ⁹
Val	4.4 × 10 ²	UV titration		18 ¹³
Lys	8.0 × 10 ²	ITC	10 mM NH ₄ OAc, pH = 6, 30°C	19 ⁹
Lys	8.7 × 10 ²	Fluorescence titration	10 mM NH ₄ OAc, pH = 6, 25°C	19 ⁹
Trp	1.6 × 10 ³	Fluorescence titration	10 mM NH ₄ OAc, pH = 6, 25°C	19 ⁹
Trp	1.9 × 10 ³	ITC	10 mM NH ₄ OAc, pH = 6, 30°C	19 ⁹
Tyr	2.2 × 10 ⁴	ITC	10 mM NH ₄ OAc, pH = 6, 30°C	19 ⁹
Tyr	2.4 × 10 ⁴	Fluorescence titration	10 mM NH ₄ OAc, pH = 6, 25°C	19 ⁹
Tyr	2.3 × 10 ⁵	UV titration		18 ⁸

Trp	3.7×10^5	UV titration		18^8
Phe	1.5×10^5	NMR titration	Water, 25 °C	$2i^{10}$
Phe	8.2×10^5	UV titration		18^8
Phe	1.8×10^6	ITC	Water, 25 °C	$2j^{11}$
1-Ad Acid	3.23×10^8	NMR		$2i^{10}$

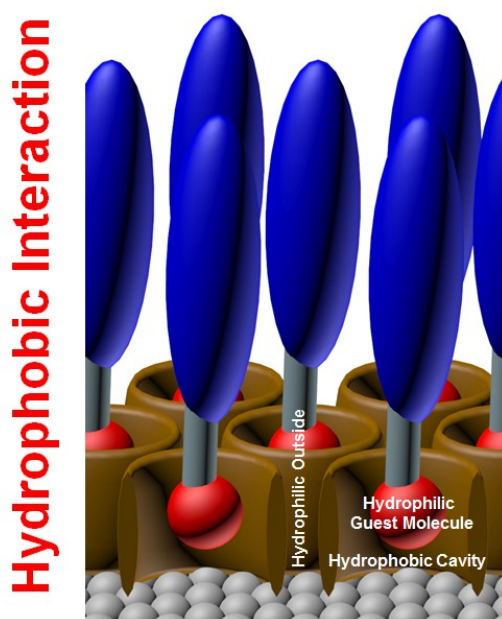


Figure S27. Binding Model of Self-Assembly.

4.8 Conjugation Amount Test

The protein concentration of CB-UCNPs@IgG-ADC was tested according to the protocol from Thermo Scientific.

4.9 Conjugation Availability

4.9.1 Conjugation Availability of CB-UCNPs

The number of CB[7] ($N_{CB[7]}$) on the surface is

$$N_{CB[7]} = \frac{m_{CB[7]}}{M_{CB[7]}} N_A$$

where $m_{CB[7]}$ is the weight of CB[7] in CB-UCNPs, was tested by TGA, $M_{CB[7]}$ is molecular weight of CB[7], N_A is Avogadro's constant.

The number of IgG (N_{IgG}) on the surface is

$$N_{IgG} = \frac{m_{IgG}}{M_{IgG}} N_A$$

where m_{IgG} is the weight of IgG in CB-UCNPs@IgG-ADC, was tested by BCA protein concentration test, $M_{IgG-ADC}$ is molecular weight of IgG, N_A is Avogadro's constant.

So, the conjugation availability is

$$conjugation\ availability = \frac{N_{IgG}}{N_{CB[7]}} \times 100\%$$

We calculated the conjugation availability of CB-UCNPs with IgG is 7.5%.

4.9.2 Conjugation Availability of UCNPs-COOH

The same as CB-UCNPs, the conjugation availability of UCNPs-COOH is

$$conjugation\ availability = \frac{N_{IgG}}{N_{COOH}} \times 100\%$$

We calculated the conjugation availability of CB-UCNPs with IgG is 1.7%.

4.10 Conjugation Rate of Self-Assembly

The process of self-assembly is shown above. The samples were collected at the different time pots.

The concentration of protein at various times was tested by BCA protein concentration test.

4.11 The Shelf-Life of Self-Assembly Conjugation

Two experiments to investigate the shelf-life of the self-assembled conjugation system were carried out. (1) The emission stability of self-assembled CB-UCNP@IgG-ADC system, and (2) the binding

stability of IgG in the self-assembled system. After the self-assembly, the CB-UCNP@IgG-ADC was kept at 4 °C, and the emission spectrum was measured for a varied time from 0 h to 192 h (8 d). The half-life of conjugation is about 7 d (ca. 167 h). We also measured the free IgG amount in solution using BCA method after the conjugation of IgG. After 8 d, only 6.6% IgG was shown in the solution indicating the disassembly at a very slow rate. (**Table S4**, **Table S5**, **Figure S28** and **Figure S29**) The difference between Tables S4 and S5 can be explained because UCNPs can precipitate or hydrolyze even if IgG is still on their surface. In any case, the data of Table S4 is more relevant for the overall stability.

Table S4. The emission stability of CB-UCNP@IgG-ADC

Time	The Emission Percentage
12 h	(99.0±0.82)%
24 h	(94.2±0.42)%
48 h	(86.3±1.32)%
72 h	(75.3±1.79)%
96 h	(65.4±2.06)%
120 h	(58.2±1.56)%
144 h	(54.9±0.96)%
168 h	(51.5±2.52)%
192 h	(48.6±2.10)%

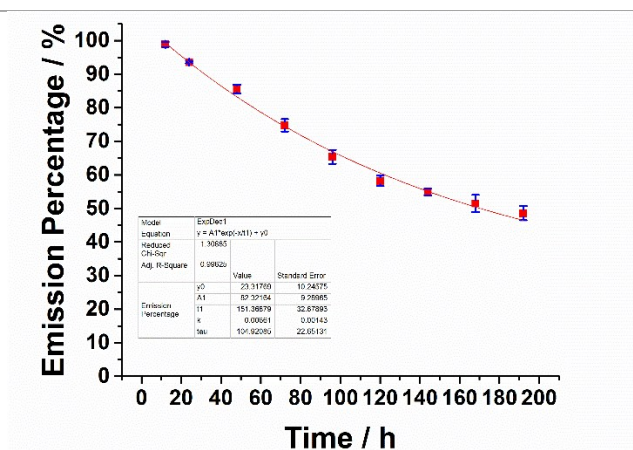
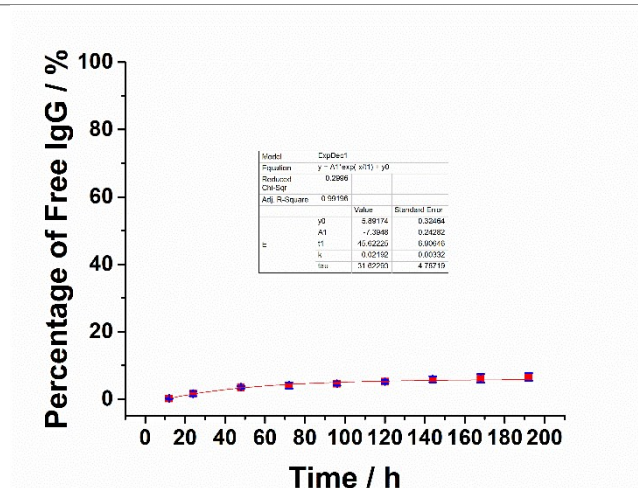


Figure S28. The emission stability of CB-UCNP@IgG-ADC.

Table S5. Free IgG percentage in media

Time	Percentage of Free IgG
12 h	(0.2±0.16)%
24 h	(1.6±0.78)%
48 h	(3.7±0.44)%
72 h	(4.3±0.83)%
96 h	(4.6±0.55)%
120 h	(5.2±0.43)%
144 h	(5.9±0.89)%
168 h	(6.2±1.25)%
192 h	(6.6±1.15)%

**Figure S29.** Free IgG percentage in media.

5 *In vitro* Cell Study

5.1 Cytotoxicity of CB-UCNPs

In vitro cytotoxicity was measured by performing Methyl Thiazolyl Tetrazolium (MTT) assays on the human cervical cancer HeLa cells. Cells were seeded into a 96-well cell culture plate at 1×10^5 /well at 37 °C and 5% CO₂ for 24 h. Different concentrations of CB-UCNPs (25, 50, 100, 200 and 400 µg/mL, diluted in DMEM) were then added to the wells. The cells were subsequently incubated for 24

h at 37 °C under 5% CO₂. After that, MTT (20 µL; 5 mg/mL) was added to each well, and the plate was incubated for an additional 4 h at 37 °C under 5% CO₂. 200 µL DMSO was added to each well after removing media. The optical density OD570 value (Abs.) of each well was measured using a multifunction microplate reader. The following formula was used to calculate the inhibition of cell growth: Cell Viability (%) = (mean of Abs. value of treatment group/mean Abs. value of control) ×100%. **Figure S30** shows that the cell viability decreased with an increasing concentration of CB-UCNPs. Although at a very high level (400 µg/mL), cells still kept good viability (more than 70%). It means that CB-UCNPs processed an excellent biocompatibility and suitable for disease detection in the future.

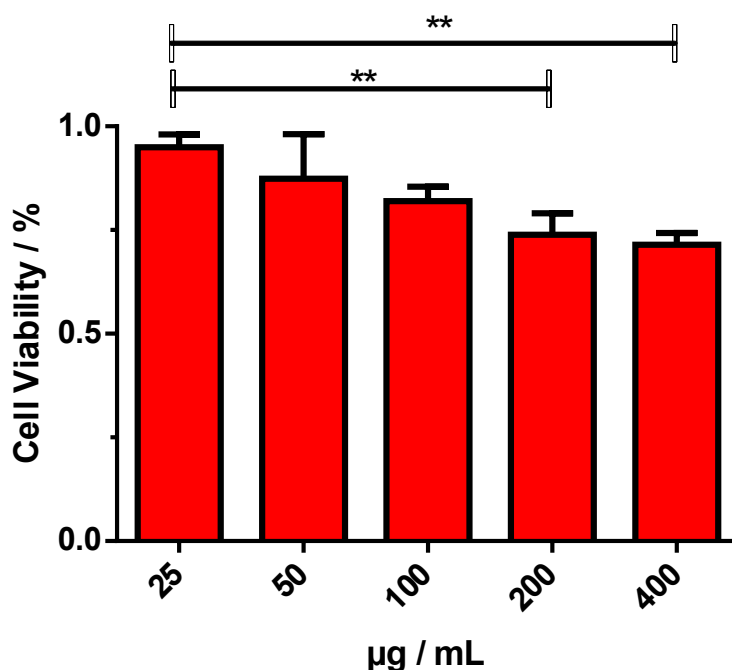


Figure S30. *In vitro* cell-growth inhibition assay for HeLa cancer cell line obtained by adding different concentrations of CB-UCNPs.

5.2 *Cell imaging*

5.2.1 **Cell culture and immunostaining**

The sample we chose for cell imaging is NaYF₄: 20% Yb, 0.5% Tm. The synthetic process is similar to the process of NaYF₄: 20% Yb, 2% Er. Human cervical cancer HeLa cells were cultured with high Dulbecco's Modified Eagle's medium (DMEM) supplemented with 10% fetal bovine serum (FBS) in a humidified incubator at 37 °C where the CO₂ level was kept constant at 5%. To do immunostaining, 1 x10⁴ HeLa cells were seeded in a confocal dish and were fixed with 4% paraformaldehyde for 15 minutes at room temperature after washing three times with PBS for 5 minutes per wash. Washing cells with PBS for three times, cells were permeabilised for 10 minutes with PBS containing 0.1% Triton X-100. The cells were then washed three times with PBS and blocked with 1% BSA in PBS for 1h at room temperature. After that, cells were washed three times with PBS and incubated in the diluted primary antibody in 1% BSA in PBS (1:500) in a humidified chamber overnight at 4°C. After three washes with PBS, cells were incubated with the diluted second antibody conjugates with UCNPs at room temperature. DAPI was used to stain nuclear for 24h at room temperature after three washes with PBS. After that, FITC conjugates of phalloidin were diluted with PBS(1:50) and used to label actin filaments in HeLa cells for 20 minutes at room temperature. Washing cell with PBS for three times, the sample was used for immunofluorescent imaging.

5.2.2 Fluorescence imaging

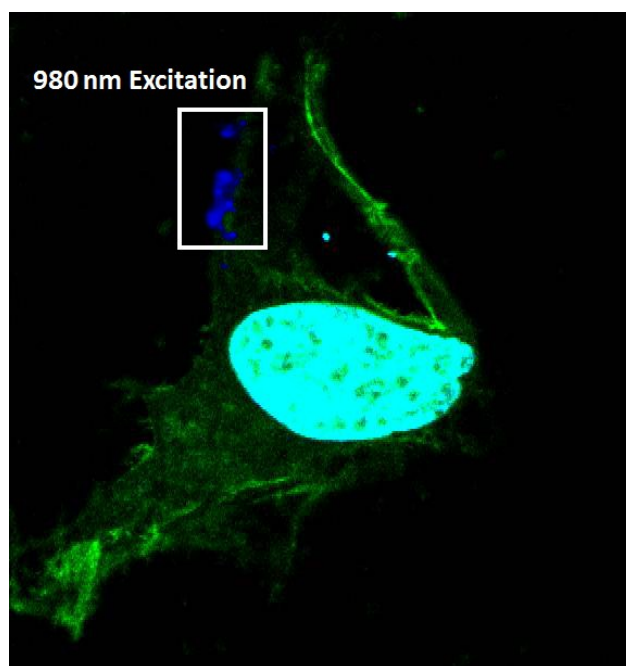


Figure S31. The cell imaging of CB-UCNP@IgG-ADC attached on the surface of HeLa cell.

All single cell imaging in confocal dishes were performed on Olympus IX 83 confocal microscopy. Samples were imaged with 20X objective lens. The DAPI and FITC conjugates of phalloidin were excited with 405 nm laser and 473 nm laser in the confocal microscopy. UCNPs on the cells were excited with 980 nm laser in wide field with another light path which was inserted into the confocal microscopy. The images of cell and UCNPs were merged with our program. One of the key limitation of this study lies in the spot size limit of the 980nm sensor which can only detect an area between 3-5 μ m (**Figure S31**).

6 References

1. Day, A.; Arnold, A. P.; Blanch, R. J.; Snushall, B., Controlling factors in the synthesis of cucurbituril and its homologues. *J. Org. Chem.* **2001**, *66* (24), 8094-8100.
2. Kim, J.; Jung, I.-S.; Kim, S.-Y.; Lee, E.; Kang, J.-K.; Sakamoto, S.; Yamaguchi, K.; Kim, K., New Cucurbituril Homologues: Syntheses, Isolation, Characterization, and X-ray Crystal Structures of Cucurbit[n]uril (n = 5, 7, and 8). *J. Am. Chem. Soc.* **2000**, *122* (3), 540-541.
3. Lu, J.; Chen, Y.; Liu, D.; Ren, W.; Lu, Y.; Shi, Y.; Piper, J.; Paulsen, I.; Jin, D., One-Step Protein Conjugation to Upconversion Nanoparticles. *Anal. Chem.* **2015**, *87* (20), 10406-10413.
4. Liu, Y.; Purich, D. L.; Wu, C.; Wu, Y.; Chen, T.; Cui, C.; Zhang, L.; Cansiz, S.; Hou, W.; Wang, Y.; Yang, S.; Tan, W., Ionic Functionalization of Hydrophobic Colloidal Nanoparticles To Form Ionic Nanoparticles with Enzymelike Properties. *J. Am. Chem. Soc.* **2015**, *137* (47), 14952-8.
5. Fragoso, A.; Caballero, J.; Almirall, E.; Villalonga, R.; Cao, R., Immobilization of Adamantane-Modified Cytochrome c at Electrode Surfaces through Supramolecular Interactions. *Langmuir* **2002**, *18* (13), 5051-5054.
6. Liu, D. M.; Xu, X. X.; Du, Y.; Qin, X.; Zhang, Y. H.; Ma, C. S.; Wen, S. H.; Ren, W.; Goldys, E. M.; Piper, J. A.; Dou, S. X.; Liu, X. G.; Jin, D. Y., Three-dimensional controlled growth of monodisperse sub-50 nm heterogeneous nanocrystals. *Nat. Commun.* **2016**, *7*, 8.
7. Moeller, T.; Martin, D. F.; Thompson, L. C.; Rerrús, R.; Feistel, G. R.; Randail, W. J., The Coordination Chemistry of Yttrium and the Rare Earth Metal Ions. *Chem. Rev.* **1965**, *65* (1), 1-50.
8. Cong, H.; Tao, L.-L.; Yu, Y.-H.; Yang, F.; Du, Y.; Xue, S.-F.; Tao, Z., Molecular Recognition of Aminoacid by Cucurbiturils. *Acta Chimica Sinica* **2006**, *64* (10), 989-996.
9. Bailey, D. M.; Hennig, A.; Uzunova, V. D.; Nau, W. M., Supramolecular tandem enzyme assays for multiparameter sensor arrays and enantiomeric excess determination of amino acids. *Chemistry-A European Journal* **2008**, *14* (20), 6069-77.
10. Liu, S.; Ruspic, C.; Mukhopadhyay, P.; Chakrabarti, S.; Zavalij, P. Y.; Isaacs, L., The Cucurbit[n]uril Family: Prime Components for Self-Sorting Systems. *J. Am. Chem. Soc.* **2005**, *127* (45), 15959-15967.

11. Rekharsky, M. V.; Mori, T.; Yang, C.; Ko, Y. H.; Selvapalam, N.; Kim, H.; Sobransingh, D.; Kaifer, A. E.; Liu, S.; Isaacs, L.; Chen, W.; Moghaddam, S.; Gilson, M. K.; Kim, K.; Inoue, Y., A synthetic host-guest system achieves avidin-biotin affinity by overcoming enthalpy-entropy compensation. *Proceedings of the National Academy of Sciences of the United States of America* **2007**, *104* (52), 20737-42.
12. Harada, A.; Kobayashi, R.; Takashima, Y.; Hashidzume, A.; Yamaguchi, H., Macroscopic self-assembly through molecular recognition. *Nature chemistry* **2011**, *3* (1), 34-7.
13. Cao, R.; Villalonga, R.; Fragoso, A., Towards nanomedicine with a supramolecular approach: a review. *IEE proceedings. Nanobiotechnology* **2005**, *152* (5), 159-64.